HHS Public Access

Author manuscript

Nat Biotechnol. Author manuscript; available in PMC 2013 January 01.

Published in final edited form as:

Nat Biotechnol. ; 30(7): 715–720. doi:10.1038/nbt.2249.

Combined small molecule inhibition accelerates developmental timing and converts human pluripotent stem cells into nociceptors

Stuart M. Chambers[1,2,*], **Yuchen Qi**[1,2,3], **Yvonne Mica**[1,2,4], **Gabsang Lee**[1,2], **Xin-Jun Zhang**[2], **Lei Niu**[2], **James Bilsland**[5], **Lishuang Cao**[5], **Edward Stevens**[5], **Paul Whiting**[5], **Song-Hai Shi**[2], and **Lorenz Studer**[1,2,6,*]

[1]Center for Stem Cell Biology, Sloan-Kettering Institute, 1275 York Ave, New York, New York 10065, USA

[2]Developmental Biology Program, Sloan-Kettering Institute, 1275 York Ave, New York, New York 10065, USA

[3]Cell & Developmental Biology, Weill Cornell Graduate School of Medical Sciences, Cornell University, New York, New York 10065, USA

[4]Gerstner Sloan-Kettering Graduate School of Biomedical Sciences, Sloan-Kettering Institute, 1275 York Ave, New York, New York 10065, USA

[5]Neusentis, Pfizer Global Research and Development, The Portway Building, Granta Park, Great Abington, Cambridge CB21 6GS, UK

[6]Department of Neurosurgery, Sloan-Kettering Institute, 1275 York Ave, New York, New York 10065, USA

Abstract

There has been considerable progress in identifying signaling pathways directing the differentiation of human pluripotent stem cells (hPSCs) into specialized cell types including neurons. However, extrinsic factor-based differentiation of hPSCs is a slow, step-wise process mimicking the protracted timing of normal human development.

Using a small molecule screen we identified a combination of five small molecule pathway inhibitors sufficient to yield hPSC-derived neurons at >75% efficiency within 10 days of differentiation. The resulting neurons express canonical markers and functional properties of human nociceptors including TTX-resistant, SCN10A-dependent sodium currents and response to nociceptive stimuli including ATP and capsaicin. Neuronal fate acquisition occurs three-fold faster than during *in vivo*[1] development suggesting that use of small molecule pathway inhibitors could develop into a general strategy for accelerating developmental timing *in vitro*. The quick

*Correspondence: Dr. Lorenz Studer, Center for Stem Cell Biology, Developmental Biology, 1275 York Ave, Box 256, New York, NY 10065, Phone: 212-639-6126, Fax: 212-717-3642, studerl@mskcc.org; Dr. Stuart Chambers, Center for Stem Cell Biology, Developmental Biology, 1275 York Ave, Box 256, New York, NY 10065, Phone: 212-639-3006, Fax: 212-717-3642, chambers@mskcc.org.

and high efficiency derivation of nociceptors offers unprecedented access to this medically relevant cell type for studies of human pain.

The *in vitro* derivation of postmitotic neurons from hPSCs requires extended culture periods typically lasting 30 days or more[2,3]. Protracted *in vitro* differentiation of hPSCs is thought to reflect the chronology of human development *in vivo*[4]. Identifying *in vitro* strategies to overcome the slow human developmental pace is a major challenge for realizing the full potential of hPSCs in basic biology and human disease modeling[5]. Here we identified a combinatorial small molecule-based approach to rapidly coax pluripotent cells into nociceptors. Previously, we reported that dual-SMAD inhibition efficiently neuralizes hPSCs[6]. Follow up studies have reported the use of small molecules replacing Noggin[7,8], and likewise we have a BMP inhibitor[9] that can replace Noggin for neuralization of hPSCs (Fig. 1a, termed LSB for the two inhibitors LDN-193189 and SB431542). In the context of LSB, we screened candidate compounds that modulate key developmental pathways (Fig. S1) to find a combination of small molecules that accelerates acquisition of postmitotic neuron markers from hPSCs. Cells were monitored for loss of the human neuroectoderm marker PAX6[10] and induction of neuronal β3-tubulin (TUBB3, TUJ1 positive)[11] at day 10 after addition of LSB. We discovered a combination of three small molecules (SU5402, CHIR99021, and DAPT; termed 3i for three inhibitors), added on day 2 (Fig. S2), abolishes PAX6 expression and induces TUBB3 in hPSCs at day 10 of differentiation (Fig. 1b). SU5402 is a potent inhibitor of VEGF, FGF, and PDGF tyrosine kinase signaling[12], CHIR99021 can act as a WNT agonist by selectively inhibiting GSK-3β stabilizing β-catenin[13], and DAPT a γ-secretase inhibitor blocks Notch signaling[14].

Upon maturation, neurons halt mitosis and lose expression of Ki67[15] and phospho-histone H3 (pHH3)[16]. Compared to cells grown in LSB only, far fewer cells in LSB + 3i (LSB3i) expressed Ki67 and pHH3 (Fig. 1c-f), and FACS confirmed this decrease in cell cycle, starting at day 7 (Fig. S3). Intercellular FACS for Nestin, a marker of neural progenitors, and TUBB3/TUJ1 was performed to quantify the efficiency of neuronal differentiation using LSB3i (Fig. 1g). In the presence of LSB, nearly all cells express Nestin (> 95%), reflecting the high efficiency of dual-SMAD inhibition[6]. Conversely, when 3i is present, 75% of cells convert to a neuronal cell fate. Combinations of 3i treatments were examined by FACS for further mechanistic insight (Fig. 1g). Although none of the factors alone yield high numbers of TUJ1 positive neurons, CHIR99021 in concert with one of the other two factors can generate robust numbers of neurons (53% for DAPT and 58% for SU5402), indicating CHIR99021 is the key factor for inducing neuronal differentiation while SU5402 and DAPT further enhance efficiency.

We next wanted to determine if the neurons were of a particular subtype. Dual-SMAD-inhibition of hPSCs generates a PAX6 positive neuroepithelium co-expressing the anterior CNS marker FOXG1[6]. Surprisingly, we observed homogenous expression of ISL1 and BRN3A (Fig. 1h,i), canonical markers of sensory neurons[17,18] indicating the resulting neurons are of PNS rather than CNS identity at day 12. There are three major subsets of sensory neurons including proprioceptors, mechanoceptors, and nociceptors distinguished by the specific expression pattern of neurotrophic receptors [19]. Greater than 60% of all cells

expressed NTRK1 when measured by FACS at day 10 (Fig. 1l), whereas NTRK2 and NTRK3 could not be detected by immunofluorescence or FACS (Fig. S4), indicating the majority of LSB3i induced neurons are nociceptors.

Reproducibility of LSB3i treatment across additional hPSC lines including induced pluripotent stem cell (hiPSC) lines was assessed. Two hiPSC lines (C14 and C72) previously shown to efficiently neuralize[20], homogeneously gave rise to nestin positive cells when treated with LSB (>95%), and were capable of forming TUJ1 positive cells when treated with LSB3i (40% for C14 and 33% for C72; Fig. 1m). A further increase in neuronal yield was obtained upon passaging of bulk cultures (C14 in Fig. 1j,k, C72 in Fig. S5), suggesting the lower efficiency in those two hiPSC lines at day 10 is likely due to a slight delay in differentiation. Sorting on NTRK1 can be used to further enrich for BRN3A, ISL1, and TUJ1 positive neurons (Fig. S6).

Nociceptors arise via two possible lineages during human development: SOX10 positive neural crest[21,22] can generate trunk nociceptors flanking the spinal cord[23]; alternatively, head placode contributes to the trigeminal nociceptors responsible for the innervation of the face[24,25]. To discriminate between these possibilities, a transgenic *SOX10:GFP* bacterial artificial chromosome hPSC line was generated that enriches for neural crest markers within the GFP fraction (Fig. S7). GFP expression was monitored by FACS at 4, 8, 12, and 16 days after starting differentiation when the *SOX10:GFP* cells were treated with LSB, LSB and CHIR99021 (LSB/CHIR), or LSB3i (Fig. 2 a-c). A majority of cells in culture became *SOX10:GFP*+ by day 12 of differentiation when CHIR99021 was present (70% for LSB/C and 80% for LSB3i; Fig. 2d). This result indicates that the LSB3i cells adopt a neural crest identity, supporting our earlier observation that CHIR99021-mediated neural crest induction is required for the generation of LSB3i nociceptors. SU5402 accelerates neural crest cell fate choice, since LSB3i or LSB/SU/CHIR treated cells acquire neural crest identity more rapidly than LSB/CHIR and LSB/CHIR DAPT treated hPSCs (Fig. 2d, S8). To determine if *SOX10:GFP*+ cells can give rise to nociceptors, GFP+ cells at day 8 of LSB3i treatment (60% of total) were sorted and maintained in 3i until day 11 resulting again in ISL1, BRN3A, TUJ positive neurons (Fig. 2e,f). These data demonstrate that LSB3i differentiates hPSCs towards nociceptors via a SOX10+ neural crest intermediate. Immunocytochemical studies confirmed that SOX10 was never co-expressed in neuronal β3-Tubulin (TUJ1) cells. Persisting SOX10+ precursor cells (Fig. 2d) could be largely eliminated (< 5%) upon passage and replating of LSB3i cells (Fig. S9). Cells retaining *SOX10:GFP* expression, when FACS sorted by day 14, gave rise to mixed neural crest progeny (Fig. S10). In development when BRN3A is established, nociceptors uniquely express NTRK1 and RUNX1, and will differentiate into peptidergic and non-peptidergic subtypes distinguished by whether or not RUNX1 persists[19,26]. From day 8 to day 14 we observe expression of RUNX1 followed by activation of RET expression coinciding neuronal process formation (Fig. 2h). However, RUNX1 expression was extinguished by day 14 in most of the cells (Fig. 2h).

Differentiation and maturation behavior were examined to further confirm that LSB3i derived neurons were nociceptors. LSB3i nociceptors will grow long-term in N2 medium with human-beta NGF, BDNF, and GDNF. LSB3i nociceptors expressed high levels of

glutamate (Fig. 2g), consistent with an excitatory glutamatergic neuron. By day 15 peripherin was ubiquitously expressed in BRN3A/ISL1 double labeled cells (PRPH, Fig. 2i). LSB3i neurons can be cultured long-term and often organized into ganglia-like clusters by day 30 LSB3i (Fig. 2k). Expression of Substance P and CGRP was observed in > 60% of LSB3i induced neurons following sorting for NTRK1 indicating the presence of a subset of peptidergic nociceptors (Fig. 2k,l; day 30 of differentiation)[26].

Global gene expression analysis was performed (days 2, 3, 5, 7, 9, and 15, GEO accession number GSE26867) for both LSB and LSB3i treated hPSCs to characterize the timing of events during the differentiation. When select markers for neuroectoderm, neural crest, neurons, and nociceptors were examined (Table S1), distinct phases of differentiation for each could be observed (Fig. 3a). Array-based transcriptome analysis also confirmed many of our immuno-fluorescence findings (Fig. 3b,c). For instance, *ISL1*, *POU4F1 (BRN3A)*, *SOX10*, *TAC1* (pro-peptide to Substance P), *NTRK1*, *PRPH*, and *VGLUT2* were all upregulated. Conversely, we observed downregulation of *DLK1*, *LHX2*, *OTX2*, *LEFTY2*, *PAX6*, and *HES5* (Fig. 3b), all genes shown by our lab to mark hESC-derived primitive neuroectoderm[6,27]. In addition, microarray analysis provides further evidence for nociceptor intermediate cell fates, distinct from mechanoceptors and proprioceptors (Fig. S11). The neurogenin basic helix-loop-helix proteins mediate two sequential waves of neurogenesis to form the dorsal root ganglia (DRG) during mouse development[28,29]. The first wave, marked by *NEUROG2* gives rise to mechanoceptors and proprioceptors, and the second marked by *NEUROG1* gives rise to nociceptors. When hPSCs are treated with LSB, *NEUROG2* expression is strongly induced by day 7 (Fig. 3c). In contrast, hPSCs treated with LSB3i show a less pronounced induction of *NEUROG2* by day 7 but selective induction of *NEUROG1* by day 9 (Fig. 3c). We further observed that the selective nociceptor generation during LSB3i depends on continuous CHIR treatment (day 2-14). Shorter CHIR pulses (day 2-4; day 2-8) induced similar levels of *SOX10* but high expression of *ASCL1* and *NTRK1* and *NTRK2*, markers of autonomic neurons, mechanoceptors and proprioceptors respectively (Fig. S12).

Functional evidence is the ‘gold standard’ for demonstrating nociceptor identity and depends on ion channels and receptors that detect noxious stimuli[26]. We first assessed the expression of a broad range of mature nociceptive markers during LSB3i (Fig. 4a). Sodium channels SCN9A, SCN10A, and SCN11A, the purinergic receptor P2RX3 and the vanilloid receptors TRPV1 and TRPM8 were found upregulated by day 15. SCN10A is selectively expressed in both rodent and human nociceptive sensory neurons[30] and is thought to underlie the upstroke of the action potential and repetitive firing in C-fibers[31]. Using a current-voltage protocol, voltage-gated currents were observed in all LSB3i derived cells with a neuronal morphology (I = -23.7 ± 3.5 nA at 0 mV, n=30). 500 nM TTX fully blocked currents in the majority of cells (24 of 30 recordings), while 500 μM Cd^{2+} in the extracellular solution reduced the current by less than 5% (n=5), suggesting the majority of the voltage gated current is carried by Na^{+} rather than Ca^{2+}. TTX-resistant (TTX-R) currents, a characteristic feature of SCN10A-positive nociceptors, were observed (mean current amplitude = -402 ± 112 pA) in 6 cells. Application of the selective SCN10A blocker, A-803467 [32] blocked >90% of the TTX-R currents (Fig. 4b) in all cases. To further test the functional expression

of SCN10A, A-803467 was applied with action potential activity recorded in current clamp. Action potentials were detected in all cells with a neuronal morphology in response to suprathreshold current injections. In all cells with multiple action potentials, A-803467 at 500nM (n=6 cells) or 250nM (n=5 cells) decreased the repetitive firing without affecting the first action potential (Fig 4c). Similarly, A-803467 had no effect on the cells with a single action potential (Fig. S13, n=6). These data suggest that SCN10A is expressed commonly expressed in LSB3i derived neurons and contributes to the repetitive action potential firing. The expression data and functional characterization of SCN10A strongly indicates that LSB3i yields a population of neurons with a nociceptive sensory phenotype.

We further evaluated calcium flux of LSB3i nociceptors in response to 1μM capsaicin, the noxious component in chili peppers, known to activate a subset of nociceptive sensory neurons through binding to the TRPV1 vanilloid receptor[33] and to 30μM α,β Methylene-ATP, a selective agonist of P2RX3[34] mimicking inflammatory pain (Fig. 4d). α,β Methylene-ATP induced a robust calcium response. For capsaicin, we observed activation in a subset of neuronal processes and rare cell bodies (1-2% of cells), indicating either significant neurite arborization of a few responding cells or selective calcium signaling sequestered to the processes (Fig. S14). To confirm that α,β Methylene-ATP was indeed activating the P2RX3 receptor, we carried out both calcium flux (Fig. 4e, Fig. S14) and electrophysiological analyses with the selective P2RX3 antagonist A-317491[32] (Fig. 4f). Pretreatment with A-317491 significantly and in a dose-dependent manner decreased calcium flux response induced by α,β Methylene-ATP 30μM. When α,β Methylene-ATP 10 μM was focally applied to the LSB3i neurons, typical P2RX3 currents (2.1 ± 0.46 nA, n=6) with signature fast activation and fast desensitization were observed (n=6, Fig 4f). Exposure to 1 μM A-317491 blocked the current in all cells tested (average reduction of 93 .1 ± 2.3% (n=5)).

The speed with which stable, mature and functional neuronal cell fates can differentiate from hPSCs using this combined small molecule approach (Fig. S15) remains the most surprising finding. The time frame of 15 days for the generation of a functionally mature neuron phenotype is far accelerated as compared with estimates of nociceptor emergence during human development (30-50 days)[35]. Despite acceleration, hPSCs under LSB3i appear to transit through all major intermediate stages expected for generating mature nociceptors but at a much faster pace. Upregulation of ISL1 and BRN3A are concomitant with expression of SOX10, starting between days 5 and 7. The optimal time to add 3i is day 2 of dual-SMAD inhibition similar to a previous finding from our lab demonstrating an early requirement for sonic hedgehog (day 2) treatment for the effective induction of FOXA2 and human floor plate differentiation[27]. The potent role of CHIR99021 in the derivation of neural crest derived sensory neurons is likely related to activation of canonical WNT signaling, known to be essential during early neural crest specification[36], and capable of instructing naive neural crest precursors towards sensory neuron lineage[37]. We report efficient neural crest induction in the presence of the BMP-inhibitory compound LDN-193189 and the FGF-inhibitory molecule SU5402 supporting the notion that activation of WNT by CHIR rather than activation of BMPs or FGFs is critical for directing neural crest lineage in hPSCs. Previous studies in zebrafish found that Notch signaling during

neural crest development suppresses sensory neuron differentiation[38] compatible with the effects of DAPT observed our study.

The functional data in the current study confirm differentiation of hPSCs into nociceptive sensory neurons. LSB3i differentiation and growth conditions drive the cells predominantly into a *P2RX3* expressing phenotype, and some capsaicin responsive cells. This is consistent with the expression profiling data (Fig. 4a), which demonstrates stronger upregulation of *P2RX3* than *TRPV1*, and may indicate the generation of a predominant P2RX3-positive, TRPV1-negative cell type similar to the rodent non-peptidergic IB4+ population. The downregulation of Runx1 and upregulation of Ret observed between days 8 and 14 in culture are consistent with this hypothesis (Fig. 2h), and may recapitulate the switch from the NTRK1 (TrkA)-positive peptidergic population to the TrkA-negative, Ret positive non-peptidergic population observed in rodent systems[39-42]. Loss of function studies during mouse development suggest early RUNX1 expression is crucial for inducing ion channel expression and late expression is a key determinant of the non/peptidergic switch[43-45]. We report broad RUNX1 expression at day 8 and robust ion channel expression. However, once ion channel expression is established by day 15, RUNX1 levels decrease in most cells (Fig. 2h), an observation that is divergent with published RUNX1 data in the mouse. Future studies will be required to determine whether this result represents a true difference between human and rodent nociceptor development or an idiosyncrasy of our culture system.

Our combined data demonstrate that combined small molecule inhibition of endogenous signals provides rapid efficient, non-genetic, and cost-effective means to modulate hPSC cell fates. The scalable generation of hPSC-derived nociceptors using LSB3i (summarized in Table S2 and Figure S15) provides a novel platform in basic biology and drug discovery for the study of human pain perception. We envisage that strategies similar to LSB3i can be developed for the rapid induction of other neuron subtypes in the peripheral and central nervous system and may lead to a new generation of directed differentiation protocols.

Material and Methods

Cells and culture conditions

hESC lines (WA-09, passages 32-50; SHEF1,) and hiPSC lines (C14, C72; passages 10-20) were cultured with mouse embryonic fibroblasts (MEFs, Globalstem) pre-plated at 12-15,000 cells/cm^2. hiPSC lines were generated as reported[20]. Medium containing DMEM/F12, 20% knockout serum replacement, 1mM L-glutamine, 100 μM MEM non-essential amino acids, and 0.1 mM β-mercaptoethanol was made. 6ng/ml FGF-2 was added after sterile filtration and cells were fed daily and passaged weekly using 6U/mL dispase. SHEF1 cells were maintained in mTESR1 (Stem Cell Technology). The *SOX10*::*GFP* bacterial artificial chromosome cell line was generated as reported[46].

Neural and nociceptor induction

Neural induction was performed as previously reported[6]. Briefly, cells were rendered to single cells using accutase plated on gelatin for 30 minutes to remove MEFs. Non-adherent cells were collected and plated on matrigel treated dishes at a density of 20-40,000 cells/cm^2

in the presence of MEF-conditioned hESC media containing 10 ng/ml FGF-2 and 10 μM Y-27632. Neural differentiation was initiated when the cells were confluent using KSR media containing 820 ml of Knockout DMEM, 150 ml Knockout Serum Replacement, 1 mM L-glutamine, 100 μM MEM non-essential amino acids, and 0.1 mM β-mercaptoethanol. To inhibit SMAD signaling, 100nM LDN-193189 and 10 μM SB431542 were added on days 0 through 5. Cells were fed daily, and N2 media was added in increasing 25% increments every other day starting on day 4 (100% N2 on day 10). Nociceptor induction was initiated with the addition of the three inhibitors 3 μM CHIR99021, 10 μM SU5402, 10 μM DAPT on days 2 through 10. Cell passage to lower density can promote maturation of SOX10+ progenitors, and long-term culture media consisted of N2 containing 25ng/ml human-b-NGF, BDNF, and GDNF.

Microscopy, antibodies, and flow cytometry

Cells were fixed with 4% paraformaldehyde for 20 minutes, washed with PBS, permeabilized using 0.5% Triton × in PBS, and blocked using 1% BSA in PBS. For glutamate staining, .05% glutaraldehyde was added to the fixative. Primary antibodies used for microscopy included PAX6 (Covance), TUJ1 (Covance), Ki67 (Sigma), ISL1 (DSHB, Abcam), BRN3A (Millipore), RET (R&D), RUNX1 (Sigma), glutamate (Sigma), peripherin (Santa Cruz), TRPV1 (Neuromics), Substance P (Neuromics), CGRP (Neuromics), SOX10 (Santa Cruz). For flow cytometry, cells were fixed using the BD Cytofix/Cytoperm Kit (BD), including the optional 4% paraformaldehyde fixation step. Primary conjugated antibodies for flow cytometry were NTRK1-APC (R&D), Nestin-Alexa647 (BD Pharmingen), TUJ1-Alexa488 (BD Pharmingen).

Gene expression profiling

Total RNA was isolated at days 2, 3, 5, 7, 9, and 15 of differentiation of LSB or LSB3i treated hPSCs using Trizol LS. All samples were processed by the MSKCC Genomics Core Facility and hybridized to the Illumina Human 12 Oligonucleotide array. Normalization and model-based expression measurements were calculated using the Illumina analysis package (LUMI) from the Bioconductor project (www.bioconductor.org) within the statistical programming language R (http://cran.r-project.org/). Expression values are $\log_2$ of the fold change. Pair-wise comparison cut-off was significant if the multiple test corrected p-value was < 0.05.

Electrophysiology

Patch-clamp experiments were performed in whole-cell configuration at room temperature (20 - 22°C) using a Multiclamp 700B patch-clamp amplifier controlled by pClamp 10 software (Molecular Devices). Patch pipettes had resistances between 1.5 and 2 MΩ. Extracellular solution contained (mM): 140 NaCl, 4.7 KCl, 2.5 $CaCl_2$, 1.2 $MgCl_2$, 10 HEPES and 10 glucose; pH was adjusted to 7.4 with NaOH. The intracellular (pipette) solution for voltage-clamp contained (mM) 100 CsF, 45 CsCl, 10 NaCl, 1 $MgCl_2$, 10 HEPES, and 5 EGTA; pH was adjusted to 7.3 with CsOH. For current-clamp the intracellular (pipette) solution contained (mM): 130 KCl, 1 $MgCl_2$, 5 MgATP, 10 HEPES, and 0.5 EGTA; pH was adjusted to 7.3 with KOH. The osmolarity of all solutions was maintained at 320 mOsm/L for extracellular solution and 300 mOsm/L for intracellular

solutions. All chemicals were purchased from Sigma. Currents were sampled at 25 kHz and filtered at 10 kHz. Series resistance was compensated by 80-90% to reduce voltage errors, however space-clamp artifacts occurred due to the presence of processes emanating from the cell bodies. A current-voltage protocol was applied using a 20 ms pulse from -120 mV to +50 mV in 10 mV increments from a holding potential of -120 mV. The voltage protocol used to assess pharmacological block of voltage-gated sodium channels consisted of a voltage step to -85 mV for 8 seconds, a subsequent voltage step to -120mV for 100 millisecond followed by a test voltage at 0 mV for 20 ms, from a holding potential of -120 mV (Fig. 4b). Intersweep intervals were 15 seconds. Action potentials were recorded by holding the membrane potential at -60 mV and injecting increasing currents to elicit action potentials. P2× receptor currents were measured at holding potential of -80 mV. Whole-cell patch-clamp data were analyzed using Clampfit 10 (Molecular Devices) and Origin 8.1 (Originlab). Results are presented as mean ± SEM. Tests for statistical significance were performed using student *t* test or nonparametric ANOVA as noted.

Calcium imaging

For calcium imaging studies, differentiated cells at 3-4 weeks following addition of growth factors were loaded with calcium 5 dye (Molecular Devices) for 1 hour at 37°C/5% CO2. Calcium 5 dye was added at 2× stock to 100ìL DMEM/F12 1:1 medium in well. Calcium flux was monitored using the BD Pathways 855 Bioimager platform to quantify calcium flux at the single cell level.

To monitor stimulation by capsaicin or α,β-MethyleneATP, 5 basal images were taken, then compounds were added at 10× directly to medium in well to give the final stimulation concentration (capsaicin 1μM, α,β-MethyleneATP 30μM). Calcium flux was monitored for 30 seconds, with 0.3s exposure time and 0.25s delay between exposures. In a subset of wells, KCl (20mM) was added as a second stimulation to confirm the neural identity of responsive cells. For experiments using the selective P2RX3 antagonist A-317491, compound was added to wells 15 minutes prior to calcium imaging, and then the protocol was followed as above.

Following data collection, image analysis was carried out to quantify calcium flux. Segmentation was carried out based on intensity and event size. Segmentation was carried out on one control image, and held constant across all wells and images in each experiment. Calcium flux was determined by subtracting the mean basal intensity value per cell from the peak intensity following stimulation to determine the change in intensity for each individual cell.

Supplementary Material

Refer to Web version on PubMed Central for supplementary material.

Acknowledgments

We would like to thank J. Hendrikx (SKI Flow Cytometry Core lab), A. Viale (SKI Genomics Core lab), and M. Tomishima (SKI stem cell facility) for excellent technical support. We also would like to thank R. McKernan for support of functional analysis, M. Postlethwaite for assistance with electrophysiology. C. Benn for help in gene

expression analysis, and S. Kriks for assistance with hPSC culturing, The work was supported in part through grant NS066390 from NINDS/NIH and C026447 from NYSTEM to LS and C026399 from NYSTEM to SMC.

References

1. Bystron I, Rakic P, Molnar Z, Blakemore C. The first neurons of the human cerebral cortex. Nat Neurosci. 2006; 9:880–886. [PubMed: 16783367]
2. Zhang XQ, Zhang SC. Differentiation of neural precursors and dopaminergic neurons from human embryonic stem cells. Methods Mol Biol. 2009; 584:355–366. [PubMed: 19907987]
3. Elkabetz Y, et al. Human ES cell-derived neural rosettes reveal a functionally distinct early neural stem cell stage. Genes Dev. 2008; 22:152–165. [PubMed: 18198334]
4. Perrier AL, et al. Derivation of midbrain dopamine neurons from human embryonic stem cells. Proc Natl Acad Sci U S A. 2004; 101:12543–12548. [PubMed: 15310843]
5. Saha K, Jaenisch R. Technical challenges in using human induced pluripotent stem cells to model disease. Cell Stem Cell. 2009; 5:584–595. [PubMed: 19951687]
6. Chambers SM, et al. Highly efficient neural conversion of human ES and iPS cells by dual inhibition of SMAD signaling. Nat Biotechnol. 2009; 27:275–280. [PubMed: 19252484]
7. Kim DS, et al. Robust enhancement of neural differentiation from human ES and iPS cells regardless of their innate difference in differentiation propensity. Stem Cell Rev. 6:270–281. [PubMed: 20376579]
8. Zhou J, et al. High-Efficiency Induction of Neural Conversion in hESCs and hiPSCs with a Single Chemical Inhibitor of TGF-beta Superfamily Receptors. Stem Cells. 2010
9. Yu PB, et al. BMP type I receptor inhibition reduces heterotopic [corrected] ossification. Nat Med. 2008; 14:1363–1369. [PubMed: 19029982]
10. Zhang X, et al. Pax6 is a human neuroectoderm cell fate determinant. Cell Stem Cell. 2010; 7:90–100. [PubMed: 20621053]
11. Lee MK, Tuttle JB, Rebhun LI, Cleveland DW, Frankfurter A. The expression and posttranslational modification of a neuron-specific beta-tubulin isotype during chick embryogenesis. Cell Motil Cytoskeleton. 1990; 17:118–132. [PubMed: 2257630]
12. Sun L, et al. Design, synthesis, and evaluations of substituted 3-[(3- or 4-carboxyethylpyrrol-2-yl)methylidenyl]indolin-2-ones as inhibitors of VEGF, FGF, and PDGF receptor tyrosine kinases. J Med Chem. 1999; 42:5120–5130. [PubMed: 10602697]
13. Bennett CN, et al. Regulation of Wnt signaling during adipogenesis. J Biol Chem. 2002; 277:30998–31004. [PubMed: 12055200]
14. Dovey HF, et al. Functional gamma-secretase inhibitors reduce beta-amyloid peptide levels in brain. J Neurochem. 2001; 76:173–181. [PubMed: 11145990]
15. Gerdes J, Schwab U, Lemke H, Stein H. Production of a mouse monoclonal antibody reactive with a human nuclear antigen associated with cell proliferation. Int J Cancer. 1983; 31:13–20. [PubMed: 6339421]
16. Hendzel MJ, et al. Mitosis-specific phosphorylation of histone H3 initiates primarily within pericentromeric heterochromatin during G2 and spreads in an ordered fashion coincident with mitotic chromosome condensation. Chromosoma. 1997; 106:348–360. [PubMed: 9362543]
17. Sun Y, et al. A central role for Islet1 in sensory neuron development linking sensory and spinal gene regulatory programs. Nat Neurosci. 2008; 11:1283–1293. [PubMed: 18849985]
18. Gerrero MR, et al. Brn-3.0: a POU-domain protein expressed in the sensory, immune, and endocrine systems that functions on elements distinct from known octamer motifs. Proc Natl Acad Sci U S A. 1993; 90:10841–10845. [PubMed: 8248179]
19. Marmigere F, Ernfors P. Specification and connectivity of neuronal subtypes in the sensory lineage. Nat Rev Neurosci. 2007; 8:114–127. [PubMed: 17237804]
20. Papapetrou EP, et al. Stoichiometric and temporal requirements of Oct4, Sox2, Klf4, and c-Myc expression for efficient human iPSC induction and differentiation. Proc Natl Acad Sci U S A. 2009; 106:12759–12764. [PubMed: 19549847]
21. Aoki Y, et al. Sox10 regulates the development of neural crest-derived melanocytes in Xenopus. Dev Biol. 2003; 259:19–33. [PubMed: 12812785]

22. Lee G, et al. Isolation and directed differentiation of neural crest stem cells derived from human embryonic stem cells. Nat Biotechnol. 2007; 25:1468–1475. [PubMed: 18037878]
23. George L, Chaverra M, Todd V, Lansford R, Lefcort F. Nociceptive sensory neurons derive from contralaterally migrating, fate-restricted neural crest cells. Nat Neurosci. 2007; 10:1287–1293. [PubMed: 17828258]
24. Schlosser G, Northcutt RG. Development of neurogenic placodes in Xenopus laevis. J Comp Neurol. 2000; 418:121–146. [PubMed: 10701439]
25. Schlosser G. Induction and specification of cranial placodes. Dev Biol. 2006; 294:303–351. [PubMed: 16677629]
26. Woolf CJ, Ma Q. Nociceptors--noxious stimulus detectors. Neuron. 2007; 55:353–364. [PubMed: 17678850]
27. Fasano CA, Chambers SM, Lee G, Tomishima MJ, Studer L. Efficient derivation of functional floor plate tissue from human embryonic stem cells. Cell Stem Cell. 2010; 6:336–347. [PubMed: 20362538]
28. Ma Q, Fode C, Guillemot F, Anderson DJ. Neurogenin1 and neurogenin2 control two distinct waves of neurogenesis in developing dorsal root ganglia. Genes Dev. 1999; 13:1717–1728. [PubMed: 10398684]
29. Marmigere F, Ernfors P. Specification and connectivity of neuronal subtypes in the sensory lineage. Nat Rev Neurosci. 2007; 8:114–127. [PubMed: 17237804]
30. Dib-Hajj SD, et al. Two tetrodotoxin-resistant sodium channels in human dorsal root ganglion neurons. FEBS Lett. 1999; 462:117–120. [PubMed: 10580103]
31. Renganathan M, Cummins TR, Waxman SG. Contribution of Na(v)1.8 sodium channels to action potential electrogenesis in DRG neurons. J Neurophysiol. 2001; 86:629–640. [PubMed: 11495938]
32. Jarvis MF, et al. A-317491, a novel potent and selective non-nucleotide antagonist of P2×3 and P2×2/3 receptors, reduces chronic inflammatory and neuropathic pain in the rat. Proceedings of the National Academy of Sciences of the United States of America. 2002; 99:17179–17184. [PubMed: 12482951]
33. Caterina MJ, et al. The capsaicin receptor: a heat-activated ion channel in the pain pathway. Nature. 1997; 389:816–824. [PubMed: 9349813]
34. North RA. The P2X3 subunit: a molecular target in pain therapeutics. Curr Opin Investig Drugs. 2003; 4:833–840.
35. Kitao Y, Robertson B, Kudo M, Grant G. Neurogenesis of subpopulations of rat lumbar dorsal root ganglion neurons including neurons projecting to the dorsal column nuclei. J Comp Neurol. 1996; 371:249–257. [PubMed: 8835730]
36. Dorsky RI, Moon RT, Raible DW. Control of neural crest cell fate by the Wnt signalling pathway. Nature. 1998; 396:370–373. [PubMed: 9845073]
37. Lee HY, et al. Instructive role of Wnt/beta-catenin in sensory fate specification in neural crest stem cells. Science. 2004; 303:1020–1023. [PubMed: 14716020]
38. Cornell RA, Eisen JS. Delta/Notch signaling promotes formation of zebrafish neural crest by repressing Neurogenin 1 function. Development. 2002; 129:2639–2648. [PubMed: 12015292]
39. Molliver DC, et al. IB4-binding DRG neurons switch from NGF to GDNF dependence in early postnatal life. Neuron. 1997; 19:849–861. [PubMed: 9354331]
40. Ibanez CF, Ernfors P. Hierarchical control of sensory neuron development by neurotrophic factors. Neuron. 2007; 54:673–675. [PubMed: 17553418]
41. Luo W, et al. A hierarchical NGF signaling cascade controls Ret-dependent and Ret-independent events during development of nonpeptidergic DRG neurons. Neuron. 2007; 54:739–754. [PubMed: 17553423]
42. Gascon E, et al. Hepatocyte growth factor-Met signaling is required for Runx1 extinction and peptidergic differentiation in primary nociceptive neurons. J Neurosci. 2010; 30:12414–12423. [PubMed: 20844136]
43. Chen CL, et al. Runx1 determines nociceptive sensory neuron phenotype and is required for thermal and neuropathic pain. Neuron. 2006; 49:365–377. [PubMed: 16446141]

44. Kramer I, et al. A role for Runx transcription factor signaling in dorsal root ganglion sensory neuron diversification. Neuron. 2006; 49:379–393. [PubMed: 16446142]

45. Yoshikawa M, et al. Runx1 selectively regulates cell fate specification and axonal projections of dorsal root ganglion neurons. Dev Biol. 2007; 303:663–674. [PubMed: 17208218]

46. Placantonakis DG, et al. BAC transgenesis in human embryonic stem cells as a novel tool to define the human neural lineage. Stem Cells. 2009; 27:521–532. [PubMed: 19074416]

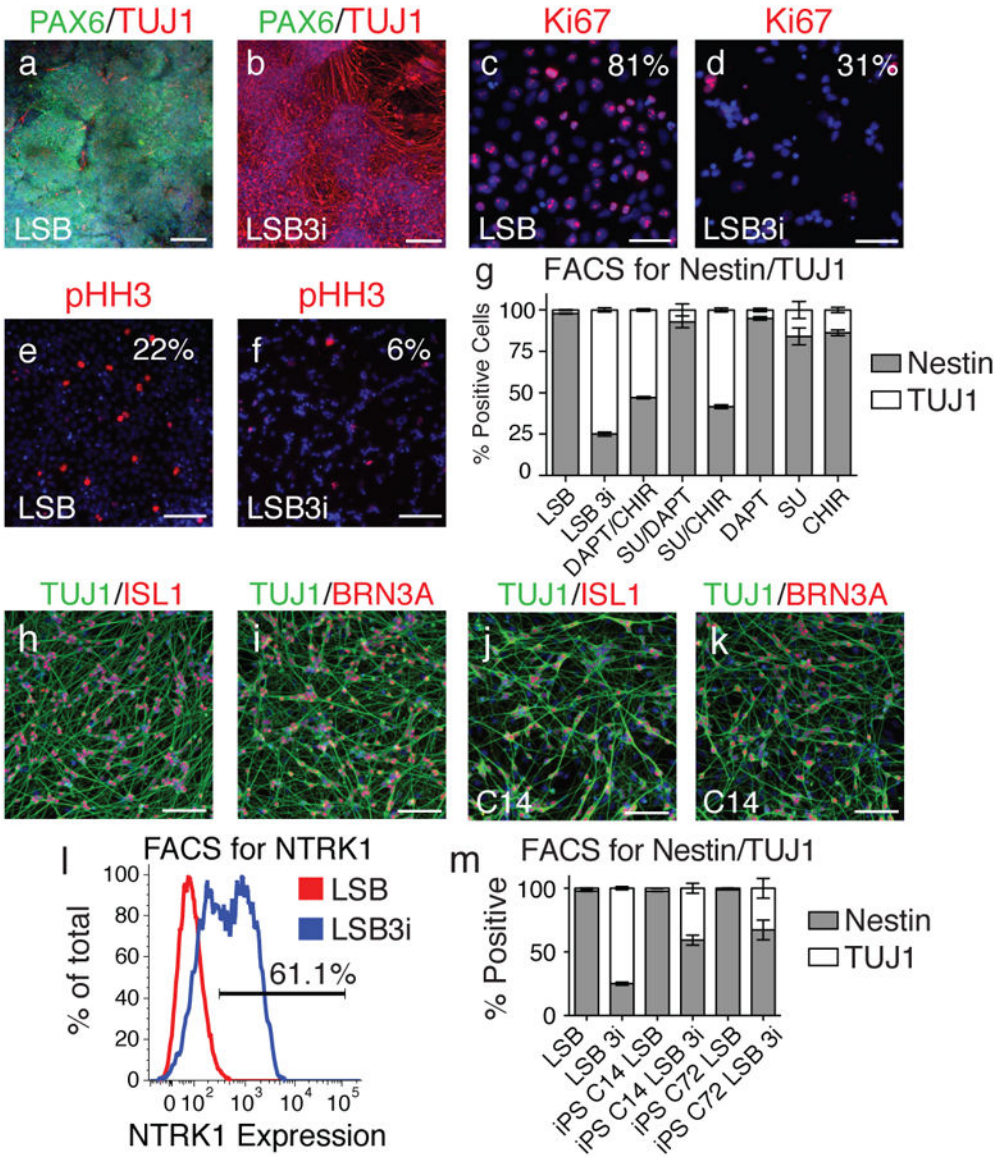

Figure 1. LSB3i treated hPSCs rapidly acquire a nociceptor phenotype within 12 days

Upon staining for TUJ1, a neuron marker, (a) compared to LSB alone, (b) far greater numbers of positive cells are observed when three inhibitors (CHIR99021, DAPT, SU5402; termed 3i) are applied 48 hours after treatment of hPSCs with LSB. Comparing expression of Ki67 and phospho-histone H3 in LSB (c,e) and LSB3i (d,f) treated hPSCs indicated a stark decline in proliferation by day 12. (g) Intracellular antibody FACS staining for Nestin and TUJ1 indicated a stark contrast in the number of neurons generated by LSB (2% TUJ1+) compared to LSB3i (75% TUJ1+). When one or two of the three inhibitors used in 3i are added, the same level of TUJ1 cells is not achieved, however CHIR with either SU5402 or DAPT can achieve greater than 53% neurons, indicating a requirement for CHIR in the formation of TUJ1+ neurons. TUJ1 positive neurons from LSB3i treated hPSCs express (h) ISL1, (i) BRN3A. (j,k) Similar neurons are observed when hiPSC lines are treated with LSB3i (C14 shown). (l) Greater than 61% of all cells express NTRK1 measured by FACS.

(m) LSB3i treated hiPSCs form neurons at a moderate efficiency. Scale bars for (a,b) are 200 μm and (c-f,h-k) are 100 μm.

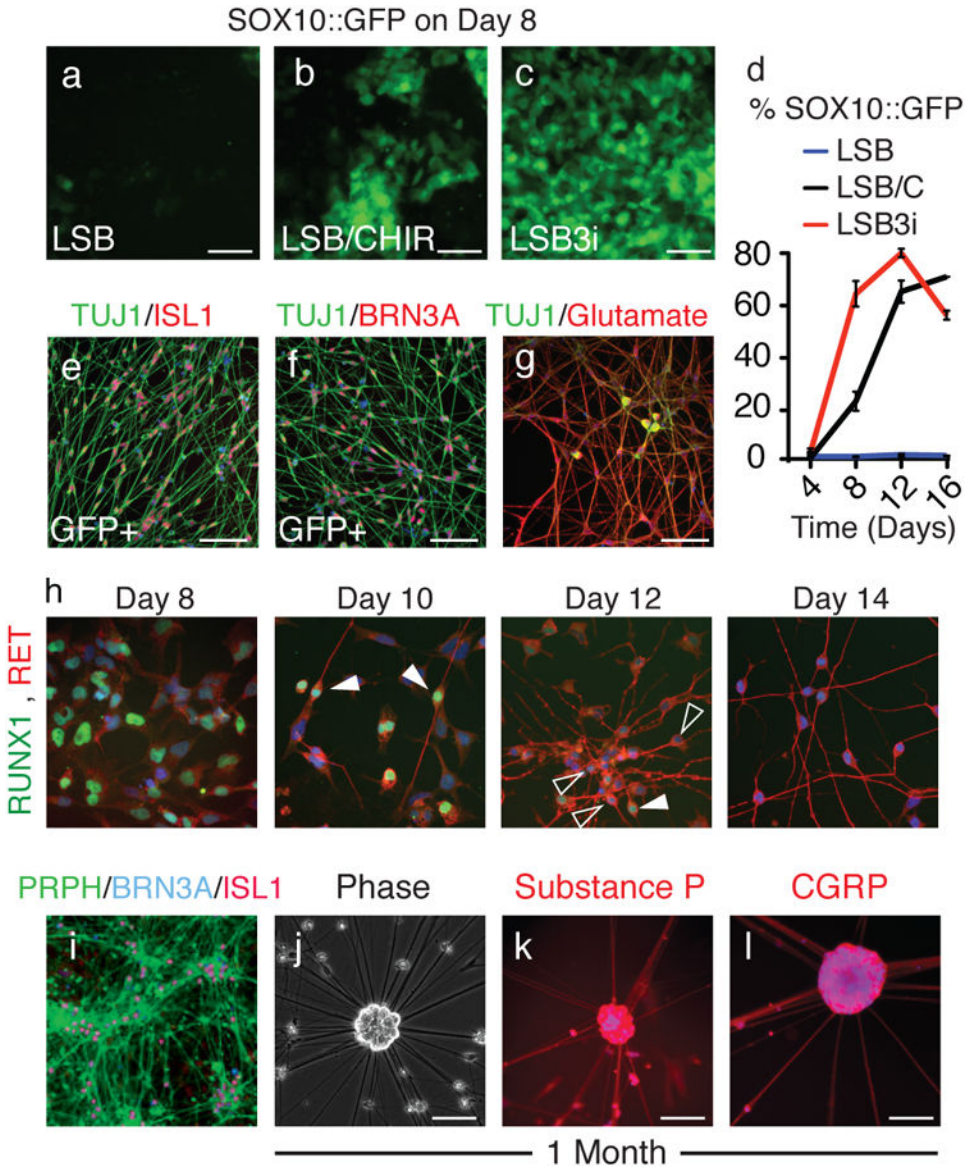

Figure 2. LSB3i treated hPSCs accelerate via a neural crest intermediate into mature bipolar nociceptors with an action potential

To monitor the emergence of neural crest stem cells, a transgenic *SOX10*: :*GFP* BAC hESC cell line was treated with (a) LSB, (b) LSB and CHIR99021, or (c) LSB3i. (d) SOX10: :GFP + expression was accelerated and maximal expression (80% GFP+ by day 12) occurred earlier compared to LSB and CHIR99021 or LSB treatment alone. Sorted SOX10: :GFP+ cells gave rise to (e) ISL1 and (f) BRN3A positive neurons. (g) LSB3i neurons stain for glutamate. (h) Between days 8 and 14 RUNX1 expression is extinguished in some of the cells (higher expression in filled arrowhead, lower in empty arrowhead) and RET upregulates. (i) By day 15, mature neurons express peripherin, and after 1 month, (j) neuronal cell bodies arrange as clusters positive for (k) Substance P and (l) CGRP. Scale bars for (a-g, i-m) are 100 μm and 50 μm for (h).

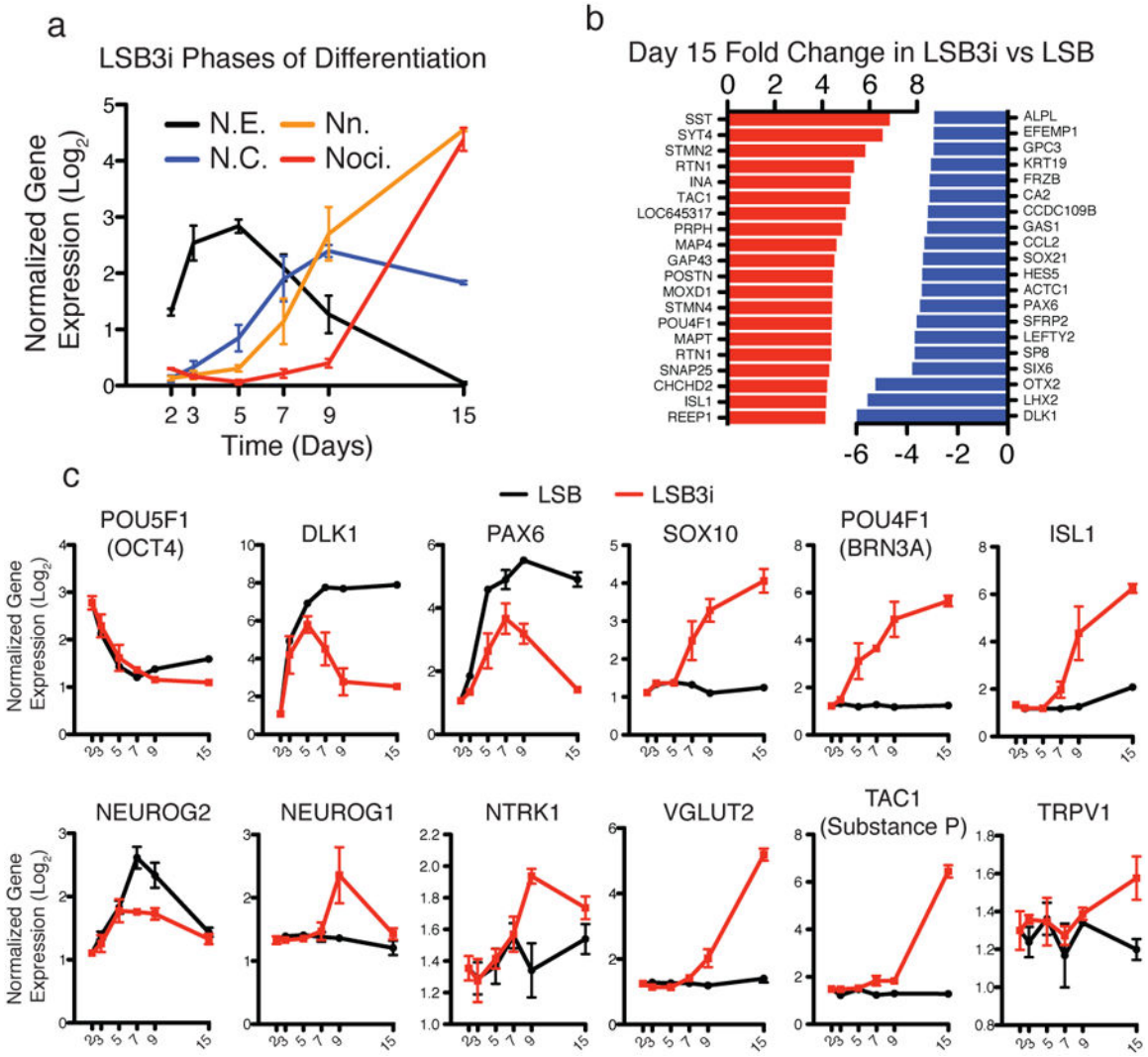

Figure 3. Gene expression of LSB3i nociceptors

Gene expression analysis was performed on days 2, 3, 5, 7, 9, and 15 for both LSB and LSB3i treated cells. (a) Distinct phases of differentiation are observed when examining markers for neuroectoderm, neural crest, neurons, and nociceptors (N.E., N.C., Nn., and Noci.). (b) Top twenty significant up- (red) and downregulated (blue) genes by fold change at day 15 for LSB3i compared to LSB. (c) Expression of *OCT4*, *DLK1*, *PAX6*, *SOX10*, *POU4F1 (BRN3A)*, *ISL1*, *NEUROG2*, *NEUROG1*, *NTRK1*, *VGLUT2*, *TAC1*, and *TRPV1* are consistent with emergence of a nociceptor.

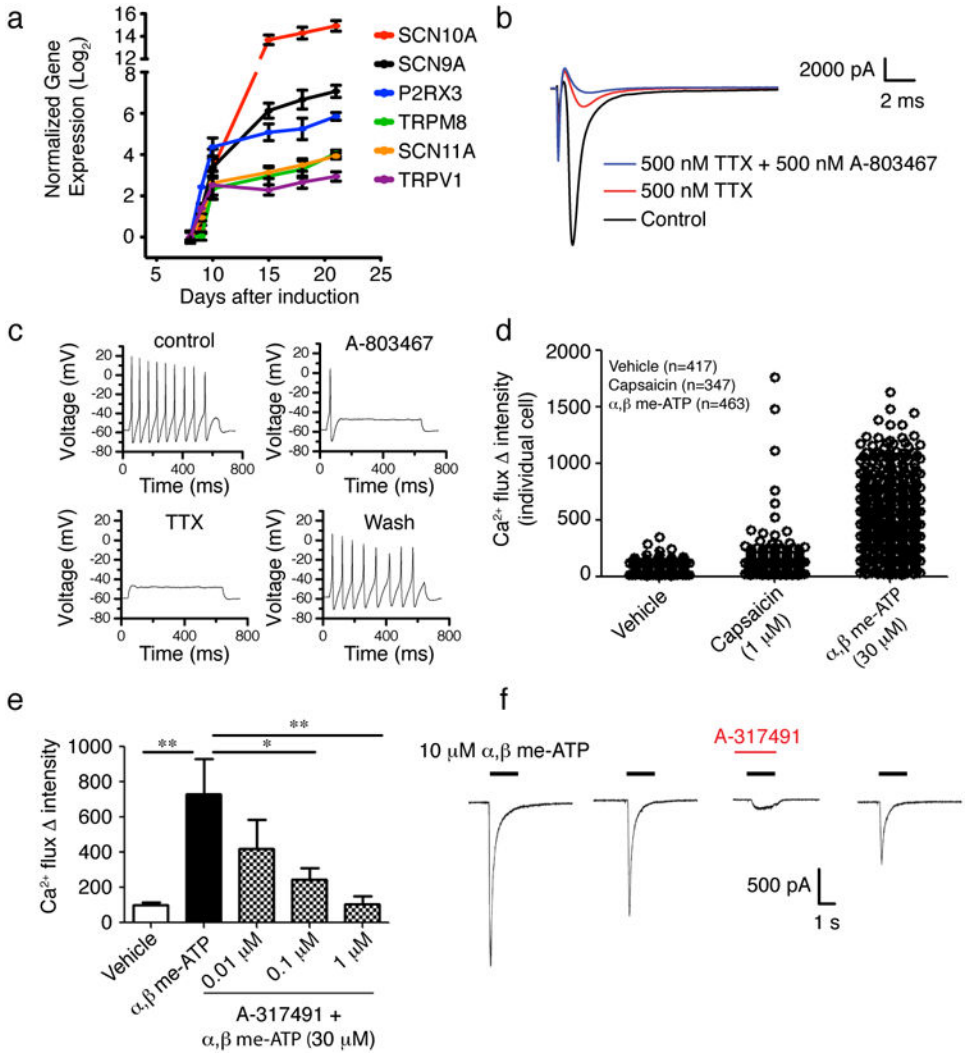

Fig. 4. Functional characterization of mature LSB3i nociceptors

(a) Time course for expression of nociceptor-specific channels and receptors during LSB3i induction and maintenance of induced neurons. (b) Example voltage-clamp recording demonstrating both TTX-S and TTX-R Na^+ currents, where the TTX-R component is further blocked by A-803467. Currents were evoked by a test pulse to 0 mV (see materials and methods). (c) A train of action potentials following current injection (75 pA). Application of 500 nM A-803467 to the same cell abolished repetitive firing with only the first action potential remaining. Additional application of 500 nM TTX blocked all action potential generation. Action potential activity recovered completely following wash-off of compounds. (d) Calcium flux induced by application of 30μM α,β Methylene ATP and 1μM capsaicin. Capsaicin induced a calcium response in 1-2% of cells, whereas a majority of LSB3i induced neurons responded to α,β Methylene ATP. To confirm that α,β Methylene ATP is acting through the P2RX3 receptor, the selective P2RX3 antagonist A-317491 was added (e). A-317491 significantly (*$p<0.05$, **$p<0.01$; one-way ANOVA, Dunnett's test) antagonized the response to α,β Methylene ATP. Electrophysiological recordings were used to analyze the current induced by α,β Methylene ATP. (f) Example of a current evoked by

10 μM α,β Methylene ATP, demonstrating typical fast activation and desensitization. The current was blocked by 1 μM A-317491 with partial recovery after wash.